The Company of **Biologists**

RESEARCH ARTICLE

Maternal B cell signaling orchestrates fetal development in mice

Mandy Busse[1], Stefanie Langwisch[1], Kerry Tedford[2], Klaus-Dieter Fischer[2] and Ana Claudia Zenclussen[1,3,4,*]

ABSTRACT

B cell participation in early embryo/fetal development and the underlying molecular pathways have not been explored. To understand whether maternal B cell absence or impaired signaling interferes with placental and fetal growth, we paired CD19-deficient (CD19−/−) mice, females with B cell-specific MyD88 (BMyD88−/−) or IL10 (BIL10−/−) deficiency as well as wild-type and MyD88−/− controls on C57Bl/6 background with BALB/c males. Pregnancies were followed by ultrasound and Doppler measurements. Implantation number was reduced in BMyD88−/− and MyD88−/− mice. Loss of MyD88 or B cell-specific deletion of MyD88 or IL10 resulted in decreased implantation areas at gestational day (gd) 5, gd8 and gd10, accompanied by reduced placental thickness, diameter and areas at gd10. Uterine artery resistance was enhanced in BIL10−/− dams at gd10. Challenge with 0.4 mg lipopolysaccharide/kg bodyweight at gd16 revealed that BMyD88−/−, BIL10−/− and CD19−/− mothers delivered preterm, whereas controls maintained their pregnancy. B cell-specific MyD88 and IL10 expression is essential for appropriate *in utero* development. IL10+B cells are involved in uterine blood flow regulation during pregnancy. Finally, B cell-specific CD19, MyD88 and IL10 expression influences susceptibility towards preterm birth.

KEY WORDS: B cells, MyD88, B10 cells, High frequency ultrasound imaging, Intrauterine development, Preterm birth, Mouse

INTRODUCTION

The modulation of the maternal immune system enables the establishment and maintenance of a pregnancy. A healthy pregnancy could be divided into three different immunologic phases: during embryo implantation, placentation and early stage of pregnancy, a pro-inflammatory milieu is present, followed by a phase of anti-inflammation during mid-pregnancy, which is replaced again by inflammation during the last trimester and end of pregnancy (Mor et al., 2017). Thus, a delicate balance between inflammatory responses and immune tolerance is essential for coordinating implantation, immune protection of semi-allogeneic fetal antigens and, at the end, parturition.

B cells contribute to fetal immune protection via different mechanisms: the most prominent ones being the production of asymmetric antibodies (AAbs) and the secretion of IL10 by so-called regulatory B cells (Breg). AAbs are antigen-specific IgGs with a mannose-rich oligosaccharide residue bound to one of the antigen-binding fragment [F(ab)] regions, which are incapable of forming antigen–antibody complexes and activate immune effector functions. Although the percentage of AAbs increases during normal pregnancy, women with recurrent pregnancy loss had significantly lower levels of AAbs (Eblen et al., 2000; Zenclussen et al., 2001). As for Breg, they have several important functions: they suppress pro-inflammatory responses by Th1 and Th17 cells, but also monocytes and dendritic cells (Rosser and Mauri, 2015), and they are also important for the maintenance of the regulatory T (Treg) cell compartment (Busse et al., 2019; Rosser and Mauri, 2015). The frequency of Breg increases in maternal peripheral blood during the first trimester of healthy pregnancies, but not in women suffering from spontaneous abortions (Rolle et al., 2013). The induction of IL10-secreting Breg is promoted by the pregnancy hormone human chorionic gonadotropin (hCG) (Fettke et al., 2016).

Another important regulatory role of B cells during pregnancy is associated with their function as professional antigen-presenting cells (APCs) (Rodriguez-Pinto, 2005). B cells express Toll-like receptors (TLR) such as TLR4 and TLR9 as well as MHC class II molecules and the costimulatory proteins CD80, CD86 and CD40. The importance of these molecules was shown by alterations in their expression in abortion-prone CBA/J×DBA/2J murine pregnancy (Lorek et al., 2019). Most TLRs require the key signaling adaptor myeloid differentiation factor 88 (MyD88) to mediate activation signals to B cells, to induce their differentiation into Breg cells and to boost antibody responses (Rawlings et al., 2012; Hou et al., 2011; Yanaba et al., 2009). MyD88-deficient mice are highly susceptible towards a broad range of bacterial and viral infections and suffer from several reproductive problems including poor reproductive performance, placentitis, metritis and peritonitis (von Bernuth et al., 2012; Villano et al., 2014). The TLR RP105 (also known as CD180) interacts with CD19 (Yazawa et al., 2003), another important B cell molecule that is required for IL10 production as it is responsible for B1 cell development; B1 cells are a main source of IL10 production (Popi et al., 2004; Sindhava et al., 2010).

In humans, the importance of B cells for pregnancy success is depicted by the observations from women whose multiple sclerosis or neuromyelitis optica spectrum disorders was treated off-level with the B cell-depleting drug Rituximab. Treatment before or during pregnancy resulted in higher rates of pregnancy complications such as spontaneous abortions and preterm births (Das et al., 2018). This reinforces the need of a clear picture as to how B cells influence pregnancy. In this regard, we have recently shown that B cell-deficient µMT mice show apparently normal pregnancies, but had smaller fetuses than wild-type (WT) controls (Busse et al., 2019). In addition, we showed that treatment of these animals with lipopolysaccharide (LPS) at doses that were harmless for controls provoked fetal loss in µMT mice, highlighting the need of fully functioning B cells for successful pregnancy (Busse et al., 2019).

DEVELOPMENT

1

During recent decades, ultrasound techniques have become integral to the practice of obstetrics. Adverse pregnancy outcomes might occur without the presence of obvious risk factors and might not have been detected by other diagnostics such as the clinical examination (Moore and Promes, 2004). Therefore, the rationale for screening all pregnancies by routine ultrasound is an early detection of the fetuses or mothers at high risk and consequently an improved management of pregnancy complications. Examples are placental pathologies, ultrasound of the cervix length to identify patients who are at risk of preterm delivery or Doppler ultrasound of umbilical artery waveforms to identify a 'compromised' fetus (Audette and Kingdom, 2018). Intrauterine growth restriction (IUGR) is still a leading cause of preventable stillbirth and is strongly associated with the obstetrical complications of iatrogenic preterm birth and preeclampsia (PE) (Nardozza et al., 2017). As rodent models are often used to mimic human pregnancy complications, such as LPS-induced preterm delivery, and to investigate potential interventions, it is important to improve the knowledge of ultrasound imaging in rodent pregnancies and the effect induced by alterations in their immune system. We have previously reported the importance of high frequency ultrasound to follow up pregnancy and understand the time points at which first deviations of normal growth are present (Meyer et al., 2017a, 2018, 2020).

The aim of the present study was to understand the impact of CD19 absence as well as B cell-specific deletion of MyD88 and IL10 on embryo and fetal growth and development *in utero*. For this, we generated B cell-specific knockout mice and followed up their pregnancy compared with the respective controls. Further, and in order to understand whether the observed changes rendered females and their fetuses more susceptible to inflammatory stress, we also analyzed the impact of LPS challenge in pregnant females whose B cells were either absent or lacking MyD88 or IL10. For this, we studied early pregnancy parameters in B cell-deficient female mice as well as in mice with B cell-specific deletion of important molecules compared with controls.

RESULTS
Abnormalities in breeding
Breeding of WT, CD19$^{-/-}$, BMyD88$^{-/-}$, MyD88$^{-/-}$ and BIL10$^{-/-}$ females with BALB/c males resulted in offspring in all combinations, only few paired dams had no detectable plug throughout the experiments (Table 1A). However, MyD88$^{-/-}$ needed much longer to show a vaginal plug compared with all other groups (P=0.0478; Table 1A). Following successful pairing of MyD88$^{-/-}$ females and BALB/c males, a significant higher rate of moribund dams due to infections/abscesses as observed at the naked eye were documented compared with WT females, where no moribund animals were observed (P=0.0087; Table 1A). In addition, non-pregnant MyD88$^{-/-}$ sentinels did not present infections or abscesses during the same period of time.

The number of implantations were determined at the end of the experiment after sacrificing the mice. The mean number of implantations in WT dams was 8.7. No significant alterations in number of implantations were found in CD19$^{-/-}$ and BIL10$^{-/-}$ dams (Table 1A). The number of implantations in BMyD88$^{-/-}$ (mean: 7.4; P=0.0055) and MyD88$^{-/-}$ (mean: 5.7; P<0.0001) was significantly decreased compared with WT mice (Table 1A), whereas the number of implantations in BIL10$^{-/-}$ was diminished but this did not reach statistical significance.

During pregnancy, by using ultrasound, we recorded the development of implantations from gestational day (gd) 5 to gd10. An implantation of a homogeneous mass without the separation between fetus and placenta and with a significantly lower volume than the other implantations within the dam was considered as a dead implantation, a fact that was also confirmed by the lack of heart beat (an exemplary picture is shown in Fig. S1A). In BIL10$^{-/-}$ females, 50% of dams carried at least one dead implantation *in uteri* compared with WT dams (P=0.0241; Table 1B), resulting in a significant higher number of dead implantations among all measured implantations (P=0.0451; Table 1B).

Table 1. Pregnancy parameters in WT, CD19$^{-/-}$, BMyD88$^{-/-}$, MyD88$^{-/-}$ and BIL10$^{-/-}$ mice
(A)

	Number of paired dams	Number of dams with plug	Time for vaginal plug	P-value (time until plug)	Number of moribund dams	P-value (moribund dams)	Number of implantations (mean)	P-value (implantations)
WT	34	34	1.9±0.8	>0.9999	0	–	8.7±1.6	–
CD19$^{-/-}$	32	31	2.0±1.0	>0.9999	0	n.s.	7.7±2.7	0.1522
BMyD88$^{-/-}$	35	33	2.0±0.8	>0.9999	0	n.s.	7.4±2.0	0.0055
MyD88$^{-/-}$	36	30	2.4±0.8	0.0478	8	0.0087	5.7±2.2	<0.0001
BIL10$^{-/-}$	9	9	1.9±0.6	>0.9999	0	n.s.	7.1±2.7	0.1487

(B)
Ultrasound measurements

	Number of measured pregnancies	Number of pregnancies with dead implantations	P-value	Number of measured implantations	Number of dead implantations	P-value
WT	8	0	–	26	0	–
CD19$^{-/-}$	3	0	–	18	0	–
BMyD88$^{-/-}$	4	0	–	22	0	–
MyD88$^{-/-}$	3	0	–	11	0	–
BIL10$^{-/-}$	6	3	0.0241	24	4	0.0451

(A) The number of total paired dams, the number of dams with a detectable plug and the time until the plug was detectable (in days; d) with the corresponding P-value. It also shows the number of moribund dams within the first 10 days of gestation and the number of implantations in WT, CD19$^{-/-}$, BMyD88$^{-/-}$, MyD88$^{-/-}$ and BIL10$^{-/-}$ dams, which was determined at the end of the experiment, with the corresponding P-values. (B) Using ultrasound, we identified the number of pregnancies having at least one dead implantation and the number of dead implantations among all measured implantations. Data are mean±s.d. The data were analyzed using the chi-square test or by Kruskal–Wallis test and Dunn's multiple comparisons test. n.s., not significant.

Female mice with modified B cell signaling had a decreased implantation area compared with WT dams

Ultrasound measurements were performed on gd5, gd8 and gd10. No differences in implantation areas were detected between WT and CD19$^{-/-}$ females at gd5 (Fig. 1A), gd8 (Fig. 1B) or gd10 (Fig. 1C). The implantations in BMyD88$^{-/-}$, MyD88$^{-/-}$ and BIL10$^{-/-}$ females were significantly smaller than in WT mice at gd5 (Fig. 1A), gd8 (Fig. 1B) and gd10 (Fig. 1C), with only few fetuses even measurable in BMyD88$^{-/-}$ and MyD88$^{-/-}$ mice at gd5. On gd10 we measured the implantation sizes as well as the sizes of the amniotic cavity which contains the fetus and grows as the fetal size increases (Fig. S1B). We found that the amniotic cavities from BMyD88$^{-/-}$, MyD88$^{-/-}$ and BIL10$^{-/-}$ dams were significantly smaller than those from WT dams (Fig. 1D). Representative pictures from implantations obtained from WT and BMyD88$^{-/-}$ mice at gd5 (I and II), gd8 (III and IV) and gd10 (V and VI) are shown in Fig. 1E.

An even more detailed classification of the implantation size is based on percentiles (Meyer et al., 2017b; Dilworth et al., 2011). Offspring smaller than the 10th percentile is defined as growth restricted, offspring smaller than the 5th percentile indicates severe growth retardation. At gd10, implantations from CD19$^{-/-}$ females were 20% growth restricted and 13.3% severely growth restricted (Fig. 1F). Of the implantations from BMyD88$^{-/-}$ females, 76.9% were severely impaired in growth, 3.8% were below the 10th

percentile. Pups from MyD88$^{-/-}$ were even more affected. In this strain, all implantations were smaller than the 5th percentile at gd10. Similarly, from BIL10$^{-/-}$ females, 89.3% of the pups were severely growth retarded, the remaining 10.7% were below the 10th percentile (dead pups excluded; Fig. 1F).

Placenta parameters were abnormal in mice with B cell-specific modifications and MyD88$^{-/-}$ mice

Next, we measured the thickness, diameter and area of placentas on gd10. Fig. 2A shows a representative picture of an implantation, divided into fetus, placenta and decidua basalis, Fig. 2B shows the measurement of the parameters thickness, diameter and area.

The placental thickness was decreased in BMyD88$^{-/-}$, MyD88$^{-/-}$ and BIL10$^{-/-}$ dams (P<0.0001 each; Fig. 2C). The diameter of the placenta was diminished in BMyD88$^{-/-}$ (P<0.0001) and BIL10$^{-/-}$ mice (P=0.0013; Fig. 2D), and the placental area was reduced in BMyD88$^{-/-}$ and BIL10$^{-/-}$ mice (P<0.0001 each; Fig. 2E) compared with the respective parameters in WT.

MyD88$^{-/-}$ and BIL10$^{-/-}$ females displayed an altered uterine artery resistance

Uteroplacental blood flow was evaluated by Doppler ultrasound at gd5, gd8 and gd10. Fig. 3A shows a representative color Doppler image of the uterine artery (UA) and Fig. 3B shows pulse-wave
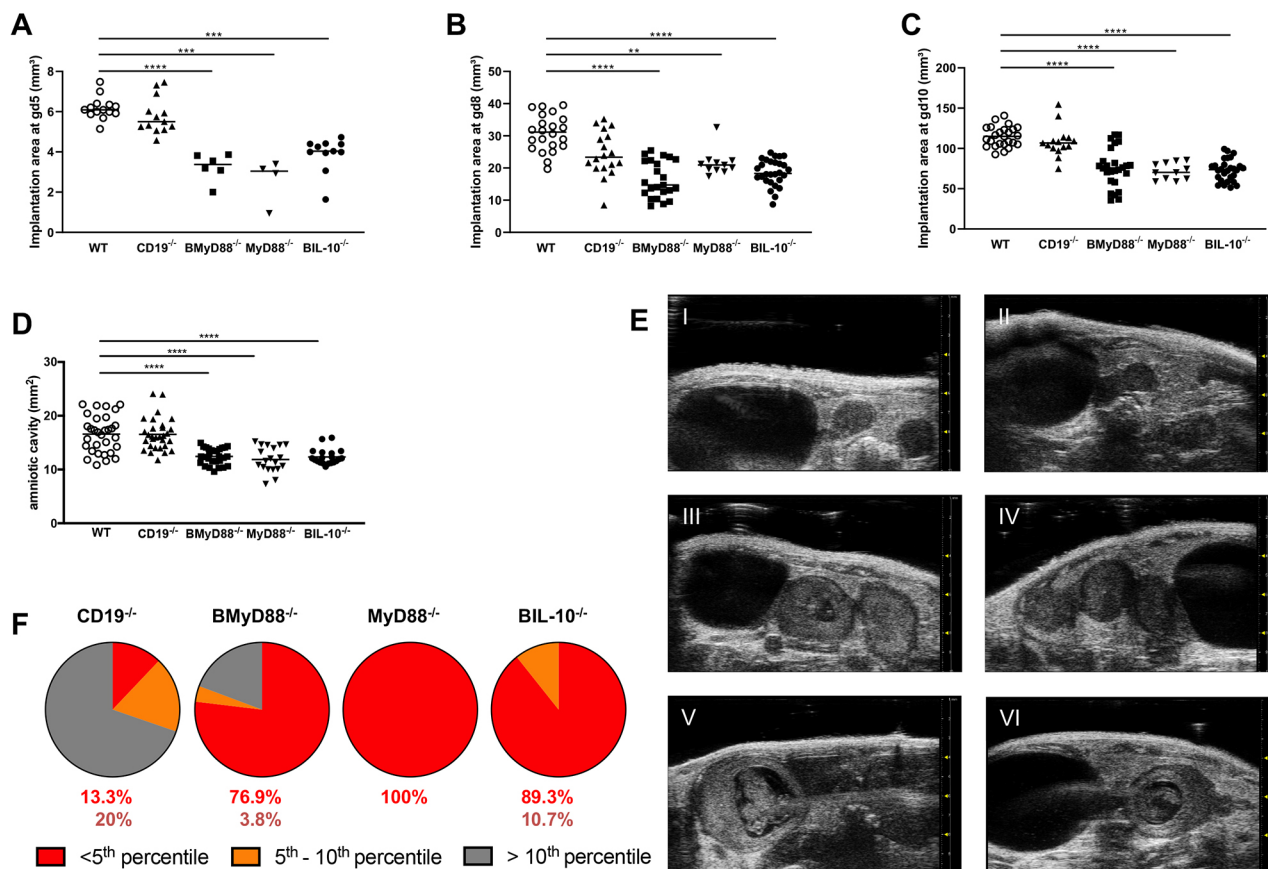
Fig. 1. Differences in the implantation area between WT, CD19$^{-/-}$, BMyD88$^{-/-}$, MyD88$^{-/-}$ and BIL10$^{-/-}$ mice. (A-C) The implantation area at gd5 (A), gd8 (B) and gd10 (C) in WT, CD19$^{-/-}$, BMyD88$^{-/-}$, MyD88$^{-/-}$ and BIL10$^{-/-}$ dams was determined using high frequency ultrasound (n=4-6 dams and n=3-11 implantations/dam per day). Dead implantations were excluded from the calculations. (D) The area of the amniotic cavity (in mm^2) at gd10. (E) Representative high-resolution images of implantations from WT (I, III and V) and BMyD88$^{-/-}$ (II, IV and IV) dams at gd5 (I and II), gd8 (III and IV) and gd10 (V and VI). (F) Percentage of gd10 implantations from CD19$^{-/-}$, BMyD88$^{-/-}$, MyD88$^{-/-}$ and BIL10$^{-/-}$ females whose weight was below the 5th percentile (red); between the 5th and the 10th percentile (orange) or above the 10th percentile (gray). Results are shown as individual values for each implantation and median; **P<0.01, ***P<0.001, ****P<0.0001 (one-way ANOVA and Holm-Sidak's multiple comparisons test or Kruskal–Wallis test and Dunn's multiple comparisons test).
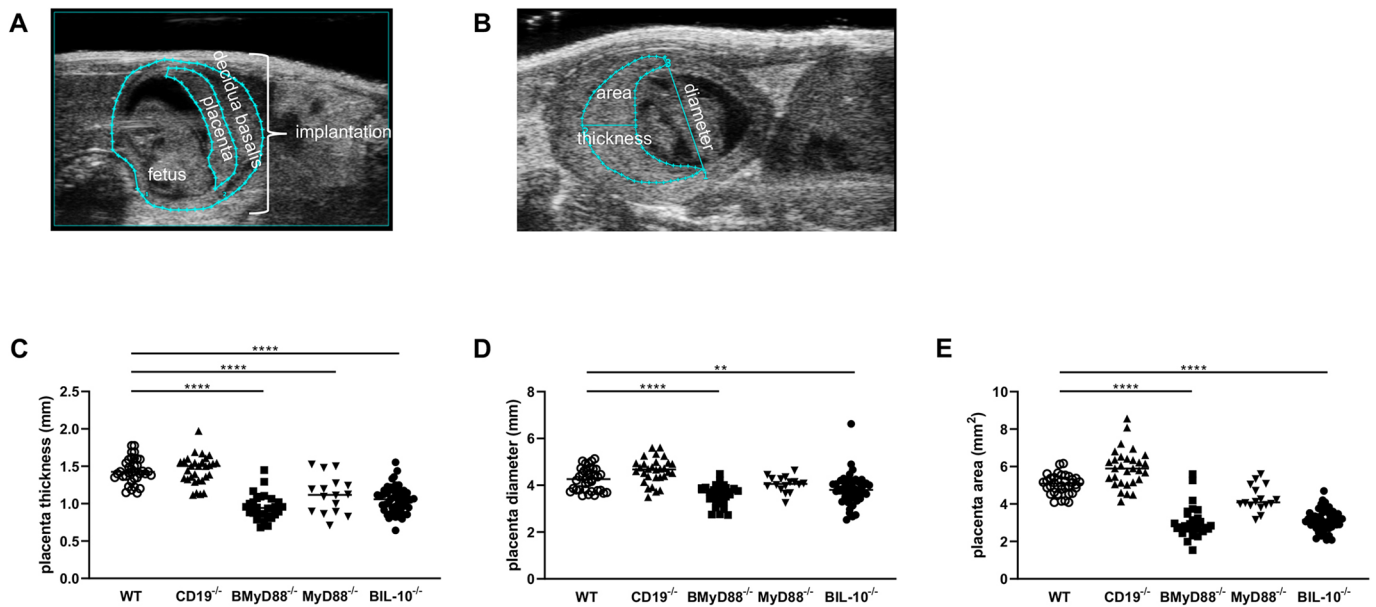
Fig. 2. Analysis of placental parameters at gd10. (A) Representative ultrasound image showing the implantation separated into embryo, placenta and decidua basalis. (B) Representative ultrasound image showing physiological placenta parameters measured included the thickness (in mm), the diameter (in mm) and the area (in mm^2). (C-E) The thickness (C), diameter (D) and area (E) of the placentae are provided as individual values for each placenta and median. n=4-6 dams/group; **$P<0.01$, ***$P<0.001$, ****$P<0.0001$ (one-way ANOVA and Dunnett's multiple comparisons test or Kruskal–Wallis test and Dunn's multiple comparisons test).

Doppler images from the UA peak systolic velocity (PS Vel) and UA end diastolic velocity (ED Vel). The Pulsatility Index (PI) and Resistance Index (RI) were calculated as described in Materials and Methods.

Although no alterations in UA PI were detected between WT, CD19$^{-/-}$, BMyD88$^{-/-}$, MyD88$^{-/-}$ and BIL10$^{-/-}$ dams (Fig. 3C), we observed augmented UA RI in MyD88$^{-/-}$ mice at gd8 compared with WT females ($P=0.0444$) and at gd10 in BIL10$^{-/-}$ dams compared with WT ($P=0.0026$), CD19$^{-/-}$ ($P=0.0022$), BMyD88$^{-/-}$ ($P=0.0387$) and MyD88$^{-/-}$ ($P=0.0122$; Fig. 3D) mice.

Deficiency in B cell-specific MyD88 or CD19 renders females more susceptible to preterm delivery following LPS challenge

Finally, we addressed the issue of whether the differences in fetal development due to defective maternal B cell signaling also influence the susceptibility towards LPS, a treatment that we employed here to induce preterm birth. LPS was injected intraperitoneally (i.p.) at different concentrations in gd16 pregnant WT, CD19$^{-/-}$, BMyD88$^{-/-}$, MyD88$^{-/-}$ and BIL10$^{-/-}$ mice. Delivery was monitored by a baby phone camera within the following 24 h and started between 16 and 19 h after LPS application. At a concentration of 1 mg LPS/kg bodyweight (BW), WT, CD19$^{-/-}$ and BMyD88$^{-/-}$ mice delivered within the observation time (Fig. 4A). WT mice did not deliver at LPS concentrations of 0.4 and 0.2 mg/kg BW (Fig. 4B,C); CD19$^{-/-}$ dams gave birth at 0.4 but not 0.2 mg LPS/kg BW, whereas BMyD88$^{-/-}$ mice delivered following i.p. injection of LPS at both 0.4 and 0.2 mg/kg BW (Fig. 4B-D). MyD88$^{-/-}$ mice did not deliver at any tested LPS concentration (Fig. 4A-C). No mouse strain gave birth within 24 h after PBS injection. These dams were sacrificed on gd17 and the pups were weighed so as to have time-mated controls. The weight of pups from BMyD88$^{-/-}$, MyD88$^{-/-}$ and BIL10$^{-/-}$ dams was significantly decreased ($P<0.0001$) compared with pups from WT dams (Fig. S2). BIL10$^{-/-}$ mice delivered at a concentration of 0.4 mg/ml BW

(Fig. 4B). As we had previously described that B cell-deficient µMT mice were also growth restricted during fetal development (Busse et al., 2019), we now address the question of whether these mice are also affected by LPS-induced preterm birth. We determined that µMT mice delivered at LPS concentrations of 0.4 and 0.2 mg/kg BW (Fig. 4B-D).

These results indicate that, except for a high LPS concentration, WT mice are protected against LPS-induced preterm birth, whereas CD19 deficiency and loss of B cell-specific MyD88 and IL10 or mature B cells enhance their susceptibility towards endotoxin-mediated preterm birth.

DISCUSSION

B cells comprise a very heterogeneous and plastic, pleiotropic population that, depending on the milieu and the situation, can undertake different functions. In order to delineate the importance of B cell function, we must generate experimental tools to study different populations separately. Besides, the importance of B cell signaling for pregnancy is not well understood. Here, we generated mice with different B cell-specific deficiencies and mated them allogeneically to mimic physiologically and immunologically relevant conditions of normal pregnancy. We analyzed intrauterine fetal growth and placenta parameters to understand the impact of B cell subpopulations under normal conditions. Our study shows that B cell-specific loss of MyD88 or IL10 influenced several aspects of the embryo and fetal development *in utero*, including diminished number of implantations, death, inappropriate fetal and placental growth and functionality of the UAs.

Several factors were identified as responsible for a lowered implantation number, among them environmental pollutants but also alterations in the immune system such as CD28 levels (Liu et al., 2014; Zhao et al., 2014). As CD28 is the essential co-stimulatory molecule for T cells, we thought about a similar function for CD19, the co-stimulator for B cells. However, as we show here, deficiency in CD19 did not influence the number of implanted embryos, and the
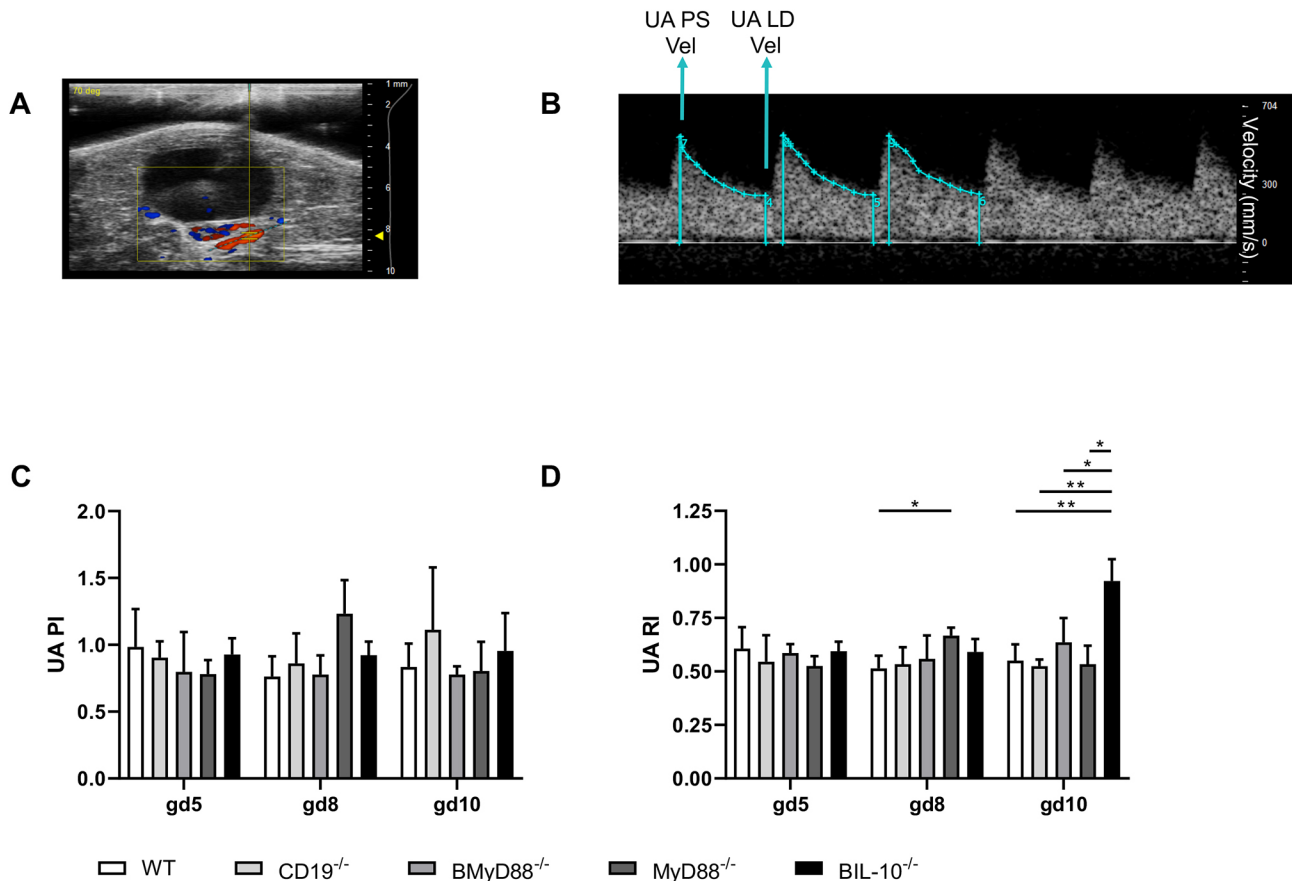
Fig. 3. Analysis of uterine artery velocities. (A) Representative color Doppler image of a uterine artery (UA). All measurements were performed at 70°. (B) Representative pulse-wave Doppler image showing UA peak systolic velocity (PS Vel) and UA end diastolic velocity (ED Vel). (C,D) The UA Pulsatility Index (PI) (C) and UA Resistance Index (RI) (D) from gd5, gd8 and gd10 are shown. Data are mean±s.d., n=3-5 dams/group; *$P<0.05$, **$P<0.01$ [two-way ANOVA (mixed effect analysis) and Tukey's multiple comparisons test].

lack of B cell-specific IL10 did not either. Loss of MyD88 in B cells, as well as the complete deficiency of MyD88, significantly decreased the implantation number. This strongly suggests that MyD88-specific signaling pathways are of utmost importance for optimal reproductive capacity in mice, and B cells contribute substantially to this process. MyD88 is used by most TLRs, which are important for host defense against infections and induction of inflammatory immune responses. The initial steps in pregnancy such as implantation are rather pro-inflammatory; deficiency of MyD88 may, however, exacerbate inflammation to a point that it hinders implantation. Inadequate TLR signaling due to MyD88 deficiency might also be responsible for the enhanced number of moribund dams seen in pregnant MyD88$^{-/-}$ females that had to be sacrificed. BIL10$^{-/-}$ dams had enhanced frequency of dead implantations. Previously, we showed the importance of IL10, produced by Treg cells, for the prevention of spontaneous abortions (Zenclussen et al., 2005), by a B1a subpopulation (Schumacher et al., 2018) and in a model of LPS-induced intrauterine fetal death in B cell-deficient mice (Busse et al., 2019). The importance of Breg for the pathology of abortion in mice has been similarly shown by others: on gd5.5, IL10-producing B cells expanded in the uterine B cell population with regulatory capacity which was shown by the suppression of proliferation and activation of syngeneic CD4+ T cells (Guzman-Genuino et al., 2019) and a decreased number of IL10 producing Breg cells were observed in abortion-prone murine breeding (Slawek et al., 2020). A diminished frequency of IL10+CD19+ B cells was also detected in peripheral blood of women with spontaneous abortions (Rolle et al., 2013). The

findings in the present paper underline the importance of IL10 during pregnancy and, in particular, of IL10-producing B cells, most probably Breg.

As we have previously observed that the implantations of B cell-deficient mice are smaller than those of WT dams (Busse et al., 2019), we now aimed to understand which molecular signaling pathways are relevant herein. We determined that the implantation areas in BIL10$^{-/-}$, BMyD88$^{-/-}$ and MyD88$^{-/-}$ animals were smaller compared with WT mice, which might be seen as IUGR.

IL10 is an important cytokine in pregnancy that influences the quality of the maternal immune response. It is expressed in the decidua and placenta, but also produced by several immune cell populations during pregnancy, among them Breg. An important process that takes place during pregnancy is the remodeling of the uterine vasculature (Osol et al., 2019; Albrecht and Pepe, 2020), located at the maternal decidua basalis, which is disturbed in maternal disorders such as IUGR and PE. Deficits in placental function or spiral artery remodeling impair fetal development (Turowski et al., 2018). We measured the RI and the PI of the UA and found an enhanced RI in BIL10$^{-/-}$ dams at gd10. Physiologically, the flow resistance in the UA strongly decreases during the first and second trimester in normal pregnancies. However, pregnancies complicated by PE or IUGR fail to decrease the flow resistance even before clinical signs of the disorders become apparent (Papageorghiou et al., 2004; Campbell et al., 1983; Garcia et al., 2016). It was also described that in an experimental model with PE resemblance, IL10 was dysregulated
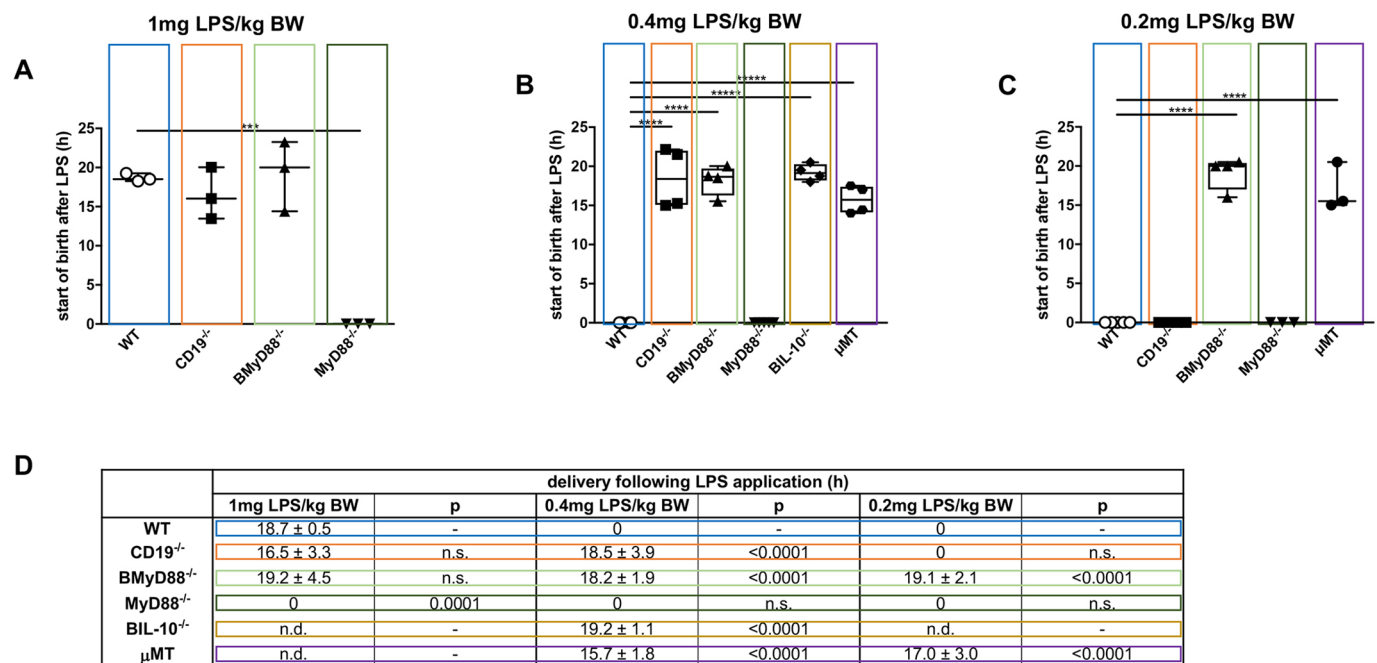
Fig. 4. Influence of B cells on LPS-induced preterm delivery. (A-C) WT, CD19$^{-/-}$, BMyD88$^{-/-}$, MyD88$^{-/-}$ and BIL10$^{-/-}$ as well as B cell-deficient µMT mice dams were treated with 1 mg LPS/kg BW (A), 0.4 mg/kg BW (B) or 0.2 mg/kg BW (C) at gd16. Data are presented as box and whiskers graph, central horizontal line indicates the median, minimum to maximum values, with each individual value as point in the graph. Preterm birth was monitored within the following 24 h. Shown is the time (h) of the delivery of the first pup. (D) Summary of delivery time (mean±s.d.; h) and the *P*-values compared with the WT group. *n*=3-5 dams/group; ***P*<0.001, *****P*<0.0001 (one-way ANOVA and Dunnett's multiple comparisons test). n.d., not done; n.s., not significant.

and the application of IL10 attenuated characteristics of the disorder such as high blood pressure and endothelial dysfunction (Chatterjee et al., 2015). Moreover, it was shown that IL10-null mutant mice have a pathologic architecture of the maternal blood sinuses and that IL10 is involved in the regulation of extravillous cytotrophoblast invasion by the inhibition of the expression of matrix metalloproteinase (Roberts et al., 2003). During pregnancy, there is an increase of proangiogenic IL10-producing T cells (Nadkarni et al., 2016). Whether B cells also exhibit proangiogenic characteristics remains to be elucidated. In a previous study, we found that IL10-expressing PC1^{high} B1a B cells rescued fetuses from rejection and decreased the frequency of IL17+ CD4+ T cells, whereas the PC1^{low} B1a population expressed significantly less IL10 and provoked fetal rejection (Schumacher et al., 2018). The present data add new knowledge, as we show that IL10-producing B cells are needed for pregnancy-compatible resistance of UAs.

Placental morphogenesis and nutrient transfer function are regulated by growth factors at the fetal-maternal interface and interferences might limit the growth of placenta and fetus (Gill et al., 2014). Therefore, we aimed to investigate the influence of B cells in placental growth and function to identify mechanisms which might affect the developing fetus. We determined that the thickness, diameter and area of the placentas in BMyD88$^{-/-}$ and BIL10$^{-/-}$ are diminished compared with WT mice. It is known that placental weight is connected to the risk of stillbirth, Apgar score and ventilation after birth (Hutcheon et al., 2012), and also with birth weight (Haeussner et al., 2013). Also, a strong correlation between placental thickness and fetal parameters such as bi-parietal diameter, femur length, abdominal circumference and thereby the estimated fetal weight, have been described (Hamdy and Ali, 2020). In addition, we found that on gd10, both placental thickness and fetal size in BMyD88$^{-/-}$, BIL10$^{-/-}$ and MyD88$^{-/-}$ mothers were decreased. A small placenta with reduced transport surface area

limits the availability of nutrients for the fetal circulation and thereby restricts the extent of fetal growth. Placental growth is regulated by genes encoding key growth factor pathway molecules (El-Hashash et al., 2010; Constancia et al., 2002), which activate signaling pathways converging on the MAPK signaling pathway. Therefore, mutations in MAPK signaling pathway proteins limit the placental growth (Hemberger and Cross, 2001; Watson and Cross, 2005). As MyD88 is an upstream regulator for the MAPK pathway (Brown et al., 2011) it is straightforward to relate that mice with a deletion in MyD88 will display the same phenotype – nevertheless this has not been previously reported.

We observed that CD19$^{-/-}$ mice had no altered embryo sizes, UA flow parameters or placental size. This indicates that despite its important function for B cell development, differentiation and maturation, loss of this protein does not influence fetal development *in utero*. Thus, we conclude that signaling pathways that are also used by other cells are relevant for B cell contribution to pregnancy establishment and fetal development.

To understand whether the negative impact of disturbed B cell signaling on fetal size and development also implied an insufficient response to inflammation, we challenged the mice with LPS. Our results demonstrate the importance of complete B cell signaling for protection against LPS-induced preterm delivery. It has been previously shown that mice with a complete MyD88 deficiency are protected against LPS-induced shock, associated with a lack of the release of pro-inflammatory mediators and of B cell activation and proliferation (Kawai et al., 1999). Here, we have shown that gd16 pregnant MyD88-deficient mice do not respond to high LPS concentrations (1 mg LPS/kg BW) that induced delivery even in WT mice. However, as MyD88 is used not only by B cells but by several immune cells for LPS signaling (Ciesielska et al., 2021), we generated B cell-specific MyD88-deficient mice to understand this particular contribution in LPS-induced preterm delivery. The effect

was the opposite, these dams were not protected but instead delivered at 0.4 mg LPS/kg BW and 0.2 mg LPS/kg BW. We observed the same susceptibility towards LPS challenge in B cell-deficient mice and mice lacking mature B cells. We have previously shown that IL10-producing Breg cells are relevant for pregnancy success in a model of LPS-induced intrauterine fetal death (Busse et al., 2019). As MyD88 is an important molecule for the generation of Breg cells following LPS stimulation (Yanaba et al., 2009), the loss of MyD88 in B cells might reduce the number of Breg cells. This might severely interfere with the proper generation of the balance between immunity and tolerance that is necessary for pregnancy success and thereby result in preterm delivery. Another possibility is that loss of B cell-specific MyD88 might result in a stronger pro-inflammatory immune response, either because other cells compensate the B cell-specific MyD88 deficiency or due to the reduction in Breg cells.

CD19-deficient dams delivered following challenge with 0.4 mg LPS/kg BW, but not after 0.2 mg LPS/kg BW treatment. Despite the fact it was shown that these mice have a profound deficiency in B1a cells (Rickert et al., 1995), and these cells exhibit regulatory function, e.g. by the production of natural IgM antibodies (Ray et al., 2015), their impact on LPS-induced preterm birth was unknown. Moreover, studies showing the influence of CD19 deficiency on LPS challenge *in vivo* are lacking. However, as CD19-deficient mice have a fully competent MyD88-signaling pathway, it further remains to be investigated whether their capacity to induce IL10-secreting Breg cells following LPS challenge is altered and whether they are able to develop an adequate pro-inflammatory response.

Taken together, our study significantly contributes to the knowledge about the role of B cells in pregnancy by showing that B cell-specific MyD88 and IL10 signaling is necessary for appropriate development *in utero*. Further, IL10 production by B cells is needed for uterine blood flow regulation during gestation. Finally, alterations in B cell-specific expression of CD19, MyD88 and IL10 enhanced susceptibility towards LPS-induced preterm delivery. Our results are important not only for understanding basic mechanisms of fetal growth, well-being and development but they are to be taken into account when designing therapeutic protocols for pregnant women.

MATERIALS AND METHODS
Animals and mouse model
C57BL/6J (H2^b) WT littermates, CD19$^{Cre/Cre}$ (referred to here as CD19$^{-/-}$; Rickert et al., 1995), MyD88$^{flox/flox}$ and MyD88$^{-/-}$ were all obtained from Jackson Laboratories. IL10$^{flox/flox}$ mice (IL10^{FL}) were provided by Axel Roers (TU Dresden, Germany; Roers et al., 2004). CD19$^{Cre/wt}$ mice were crossed with MyD88$^{flox/flox}$ or with IL10^{FL} mice to generate B cell-specific CD19$^{Cre/wt}$ MyD88$^{flox/flox}$ and CD19$^{Cre/wt}$ IL10$^{flox/flox}$ mice (referred to here as BMyD88$^{-/-}$ and BIL10$^{-/-}$, respectively) in our animal facility at the Medical University of Magdeburg. BALB/c (H2^d) males were purchased from Janvier. Animals were kept in our animal facility under optimal conditions in a 12 h light cycle. Chow and water were available *ad libitum*. Animal experiments comply with the ARRIVE guidelines and were performed according to institutional guidelines after Ministerial approval and in conformity with the European Communities Council Directive (EU Directive 2010/63/EU for animal experiments; approval number: 42502-2-1332 Uni MD and 42502-2-1327 Uni MD). Then 8-12 week old WT, BMyD88$^{-/-}$, CD19$^{-/-}$, MyD88$^{-/-}$ and BIL10$^{-/-}$ virgin female mice were allogeneically mated with BALB/c males to produce physiologically relevant pregnancies comparable with those of humans. Females were checked twice a day for the presence of vaginal plug, which indicated day 0 of pregnancy (gd0).

High frequency ultrasound imaging
Ultrasound measurements at gd5, 8 and 10 were performed using the Vevo® 2100 device (VisualSonics) in our own animal facility at the Department of

Experimental Obstetrics and Gynecology (Medical Faculty, Otto-von-Guericke University, Magdeburg). Mice were anesthetized with isoflurane (Baxter) and their paws were taped with surgical tape (3M) on the measuring electrodes of a heating platform, which was covered with electrode gel (Parker Laboratories). Electrocardiogram, body temperature and respiratory parameters were constantly monitored. The abdominal fur was removed with depilatory cream (Reckitt Benckiser), pre-warmed ultrasound gel (Gello Geltechnik) was applied on the depilated skin. The bladder was used as reference organ; the transducer (MS550D-0421, Visual Sonics) was moved starting from the bladder to the left and the right side of the abdominal cavity to identify the implantations that were present.

3D images from each implantation were recorded and 3D volume measurements were performed using VisualSonics software. The length and width from the amniotic cavity at gd10 were measured and multiplied to obtain the area (mm^2). The blood flow of the UA was visualized with Color Doppler Mode, the quantification of the blood flows through the vessels was performed with the Pulse-wave (PW) Doppler Mode. To obtain comparable results, the angle between the blood flow direction and transducer was set at 70° for the UAs. The PS Vel and ED Vel of the UAs were taken. Analysis was performed using the VisualSonics software, which calculated the RI [RI=(PS Vel − ED Vel)/PS Vel] and the PI [PI=(PS Vel − ED Vel)/velocity time integral]. After measurement the mice were placed in their cages again and after observing normal behavior post-anesthesia, they were placed back in the rack.

To identify the LPS concentration needed to induce preterm birth, dams were weighed at gd16 and subsequently injected i.p. with 1 mg LPS/kg BW, 0.2 mg LPS/kg BW or 0.4 mg LPS/kg BW in 200 μl PBS. Control dams received 200 μl PBS. Mice were monitored with a baby phone camera (BM 300, NUK) for the following 24 h. Delivery was defined as the delivery of at least one pup. At the end of the experiment (gd17) mice were sacrificed, the number of implantations determined and the fetal weight from PBS controls were measured with a micro scale (Kern & Sohn).

Data analysis and statistics
Statistical analysis was performed using GraphPad Prism 8.0 software. Normality of distribution was determined by Shapiro-Wilk test. Differences between groups were analyzed by one-way ANOVA or Kruskal–Wallis test, followed by Dunnett's, Holm-Sidak's or Dunn's multiple comparisons test. Data obtained from UA PI and UA RI measurements were analyzed by mixed-effects analysis, followed by Tukey's multiple comparisons test. Differences in pregnancy parameters were analyzed by chi-square test. Significance was defined as follows: *$P<0.05$, **$P<0.01$, ***$P<0.001$, ****$P<0.0001$.

Peer review history
The peer review history is available online at https://journals.biologists.com/dev/article-lookup/doi/10.1242/dev.199783

References
Albrecht, E. D. and Pepe, G. J. (2020). Regulation of uterine spiral artery remodeling: a review. *Reprod. Sci.* **27**, 1932-1942. doi:10.1007/s43032-020-00212-8

Audette, M. C. and Kingdom, J. C. (2018). Screening for fetal growth restriction and placental insufficiency. *Semin. Fetal. Neonatal. Med.* **23**, 119-125. doi:10.1016/j.siny.2017.11.004

DEVELOPMENT

Brown, J., Wang, H., Hajishengallis, G. N. and Martin, M. (2011). TLR-signaling networks: an integration of adaptor molecules, kinases, and cross-talk. *J. Dent. Res.* **90**, 417-427. doi:10.1177/0022034510381264

Busse, M., Campe, K. J., Nowak, D., Schumacher, A., Plenagl, S., Langwisch, S., Tiegs, G., Reinhold, A. and Zenclussen, A. C. (2019). IL-10 producing B cells rescue mouse fetuses from inflammation-driven fetal death and are able to modulate T cell immune responses. *Sci. Rep.* **9**, 9335. doi:10.1038/s41598-019-45860-2

Campbell, S., Diaz-Recasens, J., Griffin, D. R., Cohen-Overbeek, T. E., Pearce, J. M., Willson, K. and Teague, M. J. (1983). New doppler technique for assessing uteroplacental blood flow. *Lancet* **1**, 675-677. doi:10.1016/S0140-6736(83)91970-0

Chatterjee, P., Chiasson, V. L., Seerangan, G., Tobin, R. P., Kopriva, S. E., Newell-Rogers, M. K. and Mitchell, B. M. (2015). Cotreatment with interleukin 4 and interleukin 10 modulates immune cells and prevents hypertension in pregnant mice. *Am. J. Hypertens.* **28**, 135-142. doi:10.1093/ajh/hpu100

Ciesielska, A., Matyjek, M. and Kwiatkowska, K. (2021). TLR4 and CD14 trafficking and its influence on LPS-induced pro-inflammatory signaling. *Cell. Mol. Life Sci.* **78**, 1233-1261. doi:10.1007/s00018-020-03656-y

Constancia, M., Hemberger, M., Hughes, J., Dean, W., Ferguson-Smith, A., Fundele, R., Stewart, F., Kelsey, G., Fowden, A., Sibley, C. et al. (2002). Placental-specific IGF-II is a major modulator of placental and fetal growth. *Nature* **417**, 945-948. doi:10.1038/nature00819

Das, G., Damotte, V., Gelfand, J. M., Bevan, C., Cree, B. A. C., Do, L., Green, A. J., Hauser, S. L. and Bove, R. (2018). Rituximab before and during pregnancy: a systematic review, and a case series in MS and NMOSD. *Neurol Neuroimmunol Neuroinflamm* **5**, e453. doi:10.1212/NXI.0000000000000453

Dilworth, M. R., Kusinski, L. C., Baker, B. C., Renshall, L. J., Greenwood, S. L., Sibley, C. P. and Wareing, M. (2011). Defining fetal growth restriction in mice: a standardized and clinically relevant approach. *Placenta* **32**, 914-916. doi:10.1016/j.placenta.2011.08.007

Eblen, A. C., Gercel-Taylor, C., Shields, L. B., Sanfilippo, J. S., Nakajima, S. T. and Taylor, D. D. (2000). Alterations in humoral immune responses associated with recurrent pregnancy loss. *Fertil. Steril.* **73**, 305-313. doi:10.1016/S0015-0282(99)00505-1

El-Hashash, A. H., Warburton, D. and Kimber, S. J. (2010). Genes and signals regulating murine trophoblast cell development. *Mech. Dev.* **127**, 1-20. doi:10.1016/j.mod.2009.09.004

Fettke, F., Schumacher, A., Canellada, A., Toledo, N., Bekeredjian-Ding, I., Bondt, A., Wuhrer, M., Costa, S. D. and Zenclussen, A. C. (2016). Maternal and fetal mechanisms of B cell regulation during pregnancy: human chorionic gonadotropin stimulates B cells to produce IL-10 while alpha-fetoprotein drives them into apoptosis. *Front. Immunol.* **7**, 495. doi:10.3389/fimmu.2016.00495

Garcia, B., Llurba, E., Valle, L., Gomez-Roig, M. D., Juan, M., Perez-Matos, C., Fernandez, M., Garcia-Hernandez, J. A., Alijotas-Reig, J., Higueras, M. T. et al. (2016). Do knowledge of uterine artery resistance in the second trimester and targeted surveillance improve maternal and perinatal outcome? UTOPIA study: a randomized controlled trial. *Ultrasound Obstet. Gynecol.* **47**, 680-689. doi:10.1002/uog.15873

Gill, J. S., Woods, M. P., Salafia, C. M. and Vvedensky, D. D. (2014). Probability distributions for measures of placental shape and morphology. *Physiol. Meas.* **35**, 483-500. doi:10.1088/0967-3334/35/3/483

Guzman-Genuino, R. M., Eldi, P., Garcia-Valtanen, P., Hayball, J. D. and Diener, K. R. (2019). Uterine B cells exhibit regulatory properties during the peri-implantation stage of murine pregnancy. *Front. Immunol.* **10**, 2899. doi:10.3389/fimmu.2019.02899

Haeussner, E., Schmitz, C., von Koch, F. and Frank, H. G. (2013). Birth weight correlates with size but not shape of the normal human placenta. *Placenta* **34**, 574-582. doi:10.1016/j.placenta.2013.04.011

Hamdy, A. and Ali, O. A. S. (2020). Role of measurement of placental thickness and diameter at the third trimester using two dimensional ultrasound in determination of low birth weight. *Al-Azhar Int. Med. J.* **1**, 19-25.

Hemberger, M. and Cross, J. C. (2001). Genes governing placental development. *Trends Endocrinol. Metab.* **12**, 162-168. doi:10.1016/S1043-2760(01)00375-7

Hou, B., Saudan, P., Ott, G., Wheeler, M. L., Ji, M., Kuzmich, L., Lee, L. M., Coffman, R. L., Bachmann, M. F. and DeFranco, A. L. (2011). Selective utilization of Toll-like receptor and MyD88 signaling in B cells for enhancement of the antiviral germinal center response. *Immunity* **34**, 375-384. doi:10.1016/j.immuni.2011.01.011

Hutcheon, J. A., McNamara, H., Platt, R. W., Benjamin, A. and Kramer, M. S. (2012). Placental weight for gestational age and adverse perinatal outcomes. *Obstet. Gynecol.* **119**, 1251-1258.

Kawai, T., Adachi, O., Ogawa, T., Takeda, K. and Akira, S. (1999). Unresponsiveness of MyD88-deficient mice to endotoxin. *Immunity* **11**, 115-122. doi:10.1016/S1074-7613(00)80086-2

Liu, S., He, J., Chen, X., Ding, Y., Geng, Y., Wu, M., Liu, X. and Wang, Y. (2014). Costimulatory molecule CD28 participates in the process of embryo implantation in mice. *Reprod. Sci.* **21**, 686-695. doi:10.1177/1933719113512537

Lorek, D., Kedzierska, A. E., Slawek, A. and Chelmonska-Soyta, A. (2019). Expression of Toll-like receptors and costimulatory molecules in splenic B cells in a normal and abortion-prone murine pregnancy model. *Am. J. Reprod. Immunol.* **82**, e13148. doi:10.1111/aji.13148

Meyer, N., Schuler, T. and Zenclussen, A. C. (2017a). Simultaneous ablation of uterine natural killer cells and uterine mast cells in mice leads to poor vascularization and abnormal Doppler measurements that compromise fetal well-being. *Front. Immunol.* **8**, 1913. doi:10.3389/fimmu.2017.01913

Meyer, N., Woidacki, K., Knofler, M., Meinhardt, G., Nowak, D., Velicky, P., Pollheimer, J. and Zenclussen, A. C. (2017b). Chymase-producing cells of the innate immune system are required for decidual vascular remodeling and fetal growth. *Sci. Rep.* **7**, 45106. doi:10.1038/srep45106

Meyer, N., Schuler, T. and Zenclussen, A. C. (2018). High frequency ultrasound for the analysis of fetal and placental development In Vivo. *J. Vis. Exp.* **141**. doi:10.3791/58616

Meyer, N., Langwisch, S., Scharm, M. and Zenclussen, A. C. (2020). Using ultrasound to define the time point of intrauterine growth retardation in a mouse model of heme oxygenase-1 deficiencydagger. *Biol. Reprod.* **103**, 126-134. doi:10.1093/biolre/ioaa057

Moore, C. and Promes, S. B. (2004). Ultrasound in pregnancy. *Emerg. Med. Clin. North Am.* **22**, 697-722. doi:10.1016/j.emc.2004.04.005

Mor, G., Aldo, P. and Alvero, A. B. (2017). The unique immunological and microbial aspects of pregnancy. *Nat. Rev. Immunol.* **17**, 469-482. doi:10.1038/nri.2017.64

Nadkarni, S., Smith, J., Sferruzzi-Perri, A. N., Ledwozyw, A., Kishore, M., Haas, R., Mauro, C., Williams, D. J., Farsky, S. H., Marelli-Berg, F. M. et al. (2016). Neutrophils induce proangiogenic T cells with a regulatory phenotype in pregnancy. *Proc. Natl. Acad. Sci. USA* **113**, E8415-E8424. doi:10.1073/pnas.1611944114

Nardozza, L. M., Caetano, A. C., Zamarian, A. C., Mazzola, J. B., Silva, C. P., Marcal, V. M., Lobo, T. F., Peixoto, A. B. and Araujo Junior, E. (2017). Fetal growth restriction: current knowledge. *Arch. Gynecol. Obstet.* **295**, 1061-1077. doi:10.1007/s00404-017-4341-9

Osol, G., Ko, N. L. and Mandala, M. (2019). Plasticity of the maternal vasculature during pregnancy. *Annu. Rev. Physiol.* **81**, 89-111. doi:10.1146/annurev-physiol-020518-114435

Papageorghiou, A. T., Yu, C. K. and Nicolaides, K. H. (2004). The role of uterine artery Doppler in predicting adverse pregnancy outcome. *Best Pract. Res. Clin. Obstet. Gynaecol.* **18**, 383-396. doi:10.1016/j.bpobgyn.2004.02.003

Popi, A. F., Lopes, J. D. and Mariano, M. (2004). Interleukin-10 secreted by B-1 cells modulates the phagocytic activity of murine macrophages in vitro. *Immunology* **113**, 348-354. doi:10.1111/j.1365-2567.2004.01969.x

Rawlings, D. J., Schwartz, M. A., Jackson, S. W. and Meyer-Bahlburg, A. (2012). Integration of B cell responses through Toll-like receptors and antigen receptors. *Nat. Rev. Immunol.* **12**, 282-294. doi:10.1038/nri3190

Ray, A., Wang, L. and Dittel, B. N. (2015). IL-10-independent regulatory B-cell subsets and mechanisms of action. *Int. Immunol.* **27**, 531-536. doi:10.1093/intimm/dxv033

Rickert, R. C., Rajewsky, K. and Roes, J. (1995). Impairment of T-cell-dependent B-cell responses and B-1 cell development in CD19-deficient mice. *Nature* **376**, 352-355. doi:10.1038/376352a0

Roberts, C. T., White, C. A., Wiemer, N. G., Ramsay, A. and Robertson, S. A. (2003). Altered placental development in interleukin-10 null mutant mice. *Placenta* **24** Suppl A, S94-S99.

Rodriguez-Pinto, D. (2005). B cells as antigen presenting cells. *Cell. Immunol.* **238**, 67-75. doi:10.1016/j.cellimm.2006.02.005

Roers, A., Siewe, L., Strittmatter, E., Deckert, M., Schluter, D., Stenzel, W., Gruber, A. D., Krieg, T., Rajewsky, K. and Muller, W. (2004). T cell-specific inactivation of the interleukin 10 gene in mice results in enhanced T cell responses but normal innate responses to lipopolysaccharide or skin irritation. *J. Exp. Med.* **200**, 1289-1297. doi:10.1084/jem.20041789

Rolle, L., Memarzadeh Tehran, M., Morell-Garcia, A., Raeva, Y., Schumacher, A., Hartig, R., Costa, S. D., Jensen, F. and Zenclussen, A. C. (2013). Cutting edge: IL-10-producing regulatory B cells in early human pregnancy. *Am. J. Reprod. Immunol.* **70**, 448-453. doi:10.1111/aji.12157

Rosser, E. C. and Mauri, C. (2015). Regulatory B cells: origin, phenotype, and function. *Immunity* **42**, 607-612. doi:10.1016/j.immuni.2015.04.005

Schumacher, A., Ehrentraut, S., Scharm, M., Wang, H., Hartig, R., Morse, H. C., III and Zenclussen, A. C. (2018). Plasma cell alloantigen 1 and IL-10 secretion define two distinct peritoneal B1a B cell subsets with opposite functions, PC1(high) cells being protective and PC1(low) cells harmful for the growing fetus. *Front. Immunol.* **9**, 1045. doi:10.3389/fimmu.2018.01045

Sindhava, V., Woodman, M. E., Stevenson, B. and Bondada, S. (2010). Interleukin-10 mediated autoregulation of murine B-1 B-cells and its role in Borrelia hermsii infection. *PLoS ONE* **5**, e11445. doi:10.1371/journal.pone.0011445

Slawek, A., Lorek, D., Kedzierska, A. E. and Chelmonska-Soyta, A. (2020). Regulatory B cells with IL-35 and IL-10 expression in a normal and abortion-prone murine pregnancy model. *Am. J. Reprod. Immunol.* **83**, e13217. doi:10.1111/aji.13217

Turowski, G., Tony Parks, W., Arbuckle, S., Jacobsen, A. F. and Heazell, A. (2018). The structure and utility of the placental pathology report. *APMIS* **126**, 638-646. doi:10.1111/apm.12842

Villano, J. S., Rong, F. and Cooper, T. K. (2014). Bacterial infections in Myd88-deficient mice. *Comp. Med.* **64**, 110-114.

von Bernuth, H., Picard, C., Puel, A. and Casanova, J. L. (2012). Experimental and natural infections in MyD88- and IRAK-4-deficient mice and humans. *Eur. J. Immunol.* **42**, 3126-3135. doi:10.1002/eji.201242683

Watson, E. D. and Cross, J. C. (2005). Development of structures and transport functions in the mouse placenta. *Physiology* **20**, 180-193.

Yanaba, K., Bouaziz, J. D., Matsushita, T., Tsubata, T. and Tedder, T. F. (2009). The development and function of regulatory B cells expressing IL-10 (B10 cells) requires antigen receptor diversity and TLR signals. *J. Immunol.* **182**, 7459-7472. doi:10.4049/jimmunol.0900270

Yazawa, N., Fujimoto, M., Sato, S., Miyake, K., Asano, N., Nagai, Y., Takeuchi, O., Takeda, K., Okochi, H., Akira, S. et al. (2003). CD19 regulates innate immunity by the toll-like receptor RP105 signaling in B lymphocytes. *Blood* **102**, 1374-1380. doi:10.1182/blood-2002-11-3573

Zenclussen, A. C., Gentile, T., Kortebani, G., Mazzolli, A. and Margni, R. (2001). Asymmetric antibodies and pregnancy. *Am. J. Reprod. Immunol.* **45**, 289-294. doi:10.1111/j.8755-8920.2001.450504.x

Zenclussen, A. C., Gerlof, K., Zenclussen, M. L., Sollwedel, A., Bertoja, A. Z., Ritter, T., Kotsch, K., Leber, J. and Volk, H. D. (2005). Abnormal T-cell reactivity against paternal antigens in spontaneous abortion: adoptive transfer of pregnancy-induced CD4+CD25+ T regulatory cells prevents fetal rejection in a murine abortion model. *Am. J. Pathol.* **166**, 811-822. doi:10.1016/S0002-9440(10)62302-4

Zhao, Y., Chen, X., Liu, X., Ding, Y., Gao, R., Qiu, Y., Wang, Y. and He, J. (2014). Exposure of mice to benzo(a)pyrene impairs endometrial receptivity and reduces the number of implantation sites during early pregnancy. *Food Chem. Toxicol.* **69**, 244-251. doi:10.1016/j.fct.2014.04.021

DEVELOPMENT